MINISTRY OF EDUCATION AND TRAINING MINISTRY OF AGRICUL AND RURAL DEVELOPMENT
VIETNAM NATIONAL UNIVERSITY OF FORESTRY

LE HOANG ANH

RESEARCH TO IMPROVE THE DYNAMICS QUALITY OF SMALL TRUCK DIFFERENTIAL USED IN AGRICULTURE AND FORESTRY

Specialized: Mechanical Engineering Technology

Code: 62520103

SUMMARY OF THE TECHNICAL DISSERTATION

Ha Noi, 2017

Dissertation is completed at:

VIETNAM NATIONAL UNIVERSITY OF RORESTRY

Supervisors:

Asso.Pro.Ph.D Nguyen Thanh Quang

Asso.Pro.Ph.D Hoang Viet

1. The first critical person:
2. The second critical person:
3. The third critical person:

The dissertation is reported before The Council of dissertation at the University level at:

Xuan Mai, …… month ……,2017 at Vietnam National University of Forestry

Can find dissertation at:

1. National Library of Viet Nam
2. Library of Vietnam National University of Forestry

INTRODUCTION

1. The urgency of the research problem

Agroforestry is an economic and technical industry that plays an important role in protecting the environment and sustainable development of our country. For the development of agriculture and forestry, means of transportation of raw materials, commodities ... should be well-run on forestry road. However, agroforestry has many corners and roads have soft ground. In order to overcome this phenomenon, it is necessary to study Differential modifications to improve transmission efficiency, reduce friction in the Differential to to turn easily and improve the quality of Differential dynamics when vehicles work on Soft ground, low coefficient of adhesion and different on two wheels.

That is why the Doctoral Candidate selected and implemented the Doctoral thesis: "**Research to improve the dynamic quality of small truck differential used in agriculture and forestry**".

2. Objectives of the study

- Determine the effect of friction torque in the Differential on differential transmission efficiency, to improve the quality of differential kinetic when vehicles turn.
- Determine the effect of differential friction torque on traction ability, improve the quality of differential dynamics when working on agroforestry.

As a basis for proposing to change the design of differential structure, expand the scope of activities of vehicles from road to agriculture and forestry.

3. Research content

3.1. Content of theory research

Dynamic modeling to investigate vehicle differential dynamics considering friction in the differential structure operating in agroforestry.

Equation and programming to calculates the transmission efficiency of the differential through the friction losses. Suggest a friction reduction scheme to increase the differential transmission power.

Set up a mathematical model, compute the algorithm to investigate the effect of the K_δ differential locking coefficient on the traction efficiency of the truck while working on road with low adhesion coefficient.

3.2. Content of experimental research

Measurement torques at the Cardan axis, two half-shalfs on the rear axles truck operating on agroforestry. Compared the results of the distribution of torque on two half-shalfs measurements on the vehicle and the test bench with torque on two half-shalfs calculated by theorical differential dynamics.

4. The scientific and practical significance of the thesis

4.1. Significance of science

The results of research have developed a methodology for investigating the differential dynamics as a scientific basis to improve the quality of small truck dynamics to use in agriculture and forestry.

4.2. Significance of reality

Research results can be used as reference document for the design and manufacture rear axles of small truck manufactured and assembled in Vietnam.

Chapter 1
OVERVIEW

1.1. Small truck differential construction

1.1.1. Symmetry Differential

Study differential of the thesis as shown in Figure 1.1

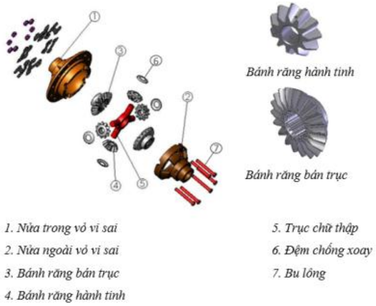

Fig. 1.1 Structure of the differential configuration of small trucks

1.1.2. Increased friction Differential

- Type of friction joint.
- Type of cylindrical gears.
- Type use Srew screw-gear.
- Type of Cam differential.
- Type of Locking differential.

1.2. The characteristics of agroforestry roads influence the operation of differential

- The agroforestry road in our country has many corners (Fig 1.2), the vehicle must be turned frequently, the differential will work harder than operating on the normal road, the friction in the differential causes damage, reduced power, reduced differential transmission efficiency, reduced vehicle revolutions. Then study to reduce friction in differential.

a) Ngoan Muc mountain, Lam Dong   b) Phuong Hoang mountain, Đăk Lăk

Figure 1.2 The forestry road taken from the satellite in the Middle region

- Sometime agriculture roads are covered with soft roads, and many bogs on the road caused vehicles often to slip, as shown in Fig 1.3. The relation of the distribution of torque in the differential [4],[17] is calculated as follows:

$$M_2 = M_4 + M_5 \qquad (1.1)$$

$$M_4 = M_5 + M_{ms} \qquad (1.2)$$

Inside:

M_4, M_5 - Torque distribution to the left and right wheels;

M_{ms} - Friction torque in differential.

When one of the two wheels falls into a bog, torque of the wheel in this side is approximately zero (assuming $M_5 = 0$). According to (1.2), $M_4 = M_{ms}$ for symmetric differential, M_{ms} has a small value, so the wheel on the hight adhesion coefficient with M_4 also not enough to win braking force to overcome. Needed the vehicle to pass, we must increase the the friction torque M_{ms} of the differential.

Fig 1.3 Bad forest road at Ngoan Muc mountain, Lam Dong

Conclusion Chapter 1

Research on improving the differential structure of the popular small trucks that can be used in agroforestry poses an urgent need for more in-depth research.

Research and analyzing the technical characteristics of the agricultural and forestry road affects the operation of the differential mechanism so that the effect of the differential friction of the differential on the vehicle's performance can be studied for Small truck on agricultural forestry road.

Chapter 2
MODELING DYNAMIC MODEL OF SMALL TRUCK DIFFERENTIAL

2.1. Small truck differential model

The torque of the drive gear M_1 via the main transmission gears and the differential will be divided into the two half-shalfs M_4, M_5. The model of small truck differential dynamics is shown in Fig 2.1.

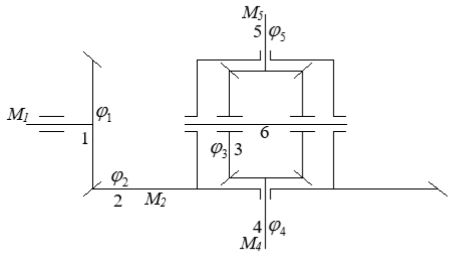

Fig 2.1 Differential dynamic model of small truck

1. Drive gear; 2. Driven gear and differential housing; 3. planetary gear; 4. Left sun gears; 5. Right sun gear; 6. Cross Axis.

φ_1, φ_2, φ_3, φ_4, φ_5 - Displacement angles of drive, driven, planetary, sun left and right gears;

M_1, M_2, M_4, M_5 - Torque on drive shaft, driven shaft, left and right half-shalf.

Using the Newton-Euler method, we set the differential equation system for describing differential dynamics when considering friction torque in differential mechanics (2.1), (2.2).

$$\begin{cases} M_1\frac{a_1}{2} - M_{Ctr} - M_1^{ms}\frac{a_1}{2} - M_2^{ms}\frac{1}{2} \pm 2M_3^{ms}a_2 \pm M_4^{ms} = (\frac{I_1a_1^2}{4} + \frac{I_2}{4} + I_4 + 2I_3a_2^2)\ddot{\varphi}_4 + (\frac{I_1a_1^2}{4} + \frac{I_2}{4} - 2I_3a_2^2)\ddot{\varphi}_5 & (2.1) \\ M_1\frac{a_1}{2} - M_{Cph} - M_1^{ms}\frac{a_1}{2} - M_2^{ms}\frac{1}{2} \pm 2M_3^{ms}a_2 \pm M_5^{ms} = (\frac{I_1a_1^2}{4} + \frac{I_2}{4} - 2I_3a_2^2)\ddot{\varphi}_4 + (\frac{I_1a_1^2}{4} + \frac{I_2}{4} + I_4 + 2I_3a_2^2)\ddot{\varphi}_5 & (2.2) \end{cases}$$

Inside:

I_1, M_1^{ms}; I_2, M_2^{ms}; I_3, M_3^{ms}; I_4, M_4^{ms}; I_5, M_5^{ms}: Is the torque of inertia and friction torque on the drive shalf, driven shalf, planetary gear shalf, sun left and right gears shalf.

2.2. Friction positions in the differential

2.2.1. Friction between planetary gear and cross shaft

The friction torque in which the planetary gear rotates around the the cross axis is the friction in the rotary joint [12], [43]. The model is shown in Figure 2.2.

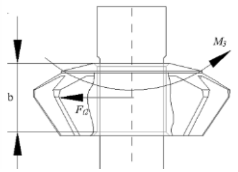

Fig 2.2 Friction model when differential gear rotates around the cross shaft

From the model we set the formula for calculating the friction torque between planetary gear and cross axis (2.3).

$$M_{ht/tr}^{ms} = \frac{\pi}{2} r_{ct} \frac{\mu_{ht/tr}}{\sqrt{1+\mu_{ht/tr}^2}} F_{t2} \qquad (2.3)$$

Inside:

$\mu_{ht/tr}$ - Friction coefficient between planetary gear and cross axis;

r_{ct} - Cross shalf radius;

F_{t2} - Force to rotate the cross axis and $F_{t2} = M_2 / 2r_{tr}$.

2.2.2. Friction between planetary gear and washer

We propose a friction study model between planetary gear and washer as shown in Fig 2.3.

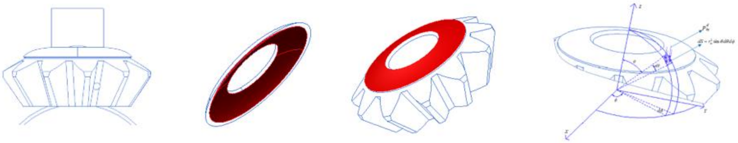

Fig 2.3 Friction torque research planetary gear and washer

The formula calculate friction torque planetary gear and washer (2.4).

$$M_{ht/d}^{ms} = \mu_{ht/d} r_{ht} F_{t2} \tan\alpha \sin\delta\left(\frac{\cos(\delta_1+\delta_0)\sin(\delta_1-\delta_0)-(\delta_1-\delta_0)}{\sin(\delta_0+\delta_1)\sin(\delta_0-\delta_1)}\right) \qquad (2.4).$$

Inside:

$\mu_{ht/d}$ - Friction coefficient between planetary gear and washer;

r_{ht} - The spherical radius of the planetary gear;

α - Meshing angle;

δ - Half-angle pitch of the planetary gear;

δ_1,δ_0 - the angles defining the spherical part of the planetary gear.

2.2.3. Friction between sun gear and differential housing

The 3D model and friction calculation model in sun gear and differential housing are shown in Fig 2.4.

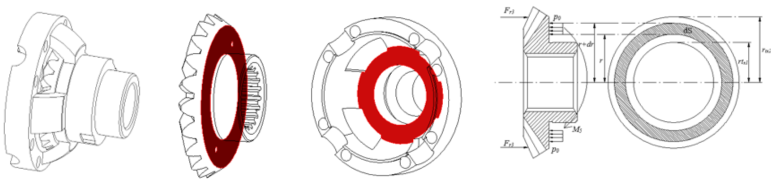

Fig 2.4 Friction study model of sun gear and differential housing

Formula calculate friction between sun gear and housing (2.5).

$$M_{bt/v}^{ms} = \frac{2}{3}\mu_{bt/v} F_{t2} \tan\alpha \sin\bar{\delta}\,\frac{(r_{tx2}^3 - r_{tx1}^3)}{(r_{tx2}^2 - r_{tx1}^2)} \qquad (2.5)$$

Inside:

$\mu_{bt/v}$ - Friction coefficient between sun gear and housing;

$\overline{\delta}$ - Half-angle pitch of the sun gear;

r_{tx1}, r_{tx2} - Radius defines the contact part between the sun gear and the housing as fig 2.4.

2.3. Influence of differential structural parameters on friction torque

2.3.1. The effect of the beveled edge length *l* on the cross axis

On the cross axis of differential on the truck, at the position attach the sun gear can be chamfered to reduce the contact pressure, Fig 2.5.

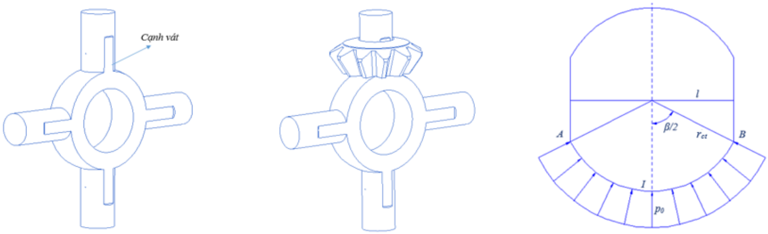

Fig 2.5 Solution of cross axis chamfered

The formula to calculate friction between cross axis and planetary gears according to the chamfer size *l* (2.6):

$$M^{ms}_{ht/tr} = \arcsin\left(\frac{l}{r_{ct}}\right) r_{ct} \frac{\mu_{ht/tr}}{\sqrt{1+\mu^2_{ht/tr}}} F_{t2} \qquad (2.6)$$

From Fig 2.6, the smaller the chamfer size *l*, the smaller friction torque $M^{ms}_{ht/tr}$. When increasing *l*, then $M^{ms}_{ht/tr}$ increase and increase fairly evenly in $l/r_{ct} = (0.5 \div 0.9)$. In the interval $l/r_{ct} = (0.9 \div 1)$, the friction torque $M^{ms}_{ht/tr}$ increases faster. We can see the relation between *l* and $M^{ms}_{ht/tr}$ are linear, thus we can decrease friction torque $M^{ms}_{ht/tr}$ by reduce the distance *l*. When reducing *l*, but if excessive reduction lead to weak axis so in the thesis choose the value *l*=0.9 r_{ct}.

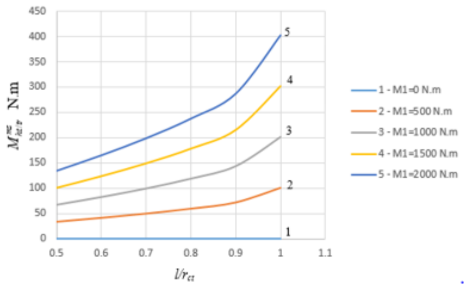

Hình 2.6 The relation l/rct and $M^{ms}_{ht/tr}$

2.3.2. Influence of drilling area on planetary gear

On the the planetary gear is drilled 5 mm, eight positions holes to reduce the contact area in the planetary gear and the washer, (Fig 2.7).

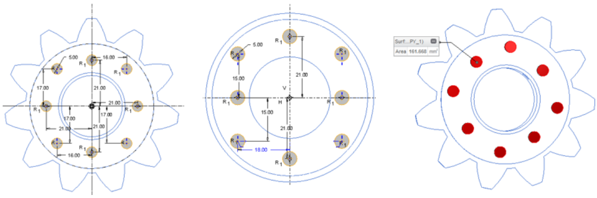

Fig 2.7 Drill plan on planetary gear

Friction torque planetary gear and washer affter drilling (2.7).

$$M^{ms}_{ht/d} = \mu_{ht/d} r_{ht} \frac{M_2}{2r_5} \tan\alpha \sin\delta \times \left(\frac{\cos(\delta_1+\delta_0)\sin(\delta_1-\delta_0)-(\delta_1-\delta_0)}{\sin(\delta_0+\delta_1)\sin(\delta_0-\delta_1)} - \frac{S^{ht}_k}{\pi r^2_{ht}\sin(\delta_0+\delta_1)\sin(\delta_0-\delta_1)} \right) \qquad (2.7)$$

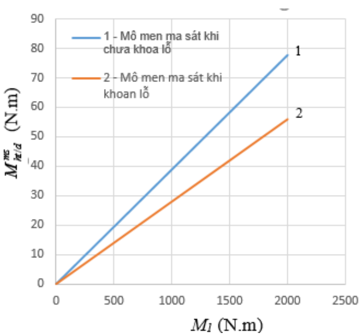

Fig 2.8 Friction torque in planetary gear and washer when not drilled and drilled

From (2.4), (2.7), a graph of the relationship torques on the drive axis M_1=[0÷2000] N.m and friction torque $M_{ht/d}^{ms}$ in the case when not drilled and drilled (Fig 2.8).

2.3.3. Influence of drilling area on sun gear

On sun gear, the differential contact section is drilled with 10 holes and the diameter is 16 mm to reduce the contact area, Fig 2.9.

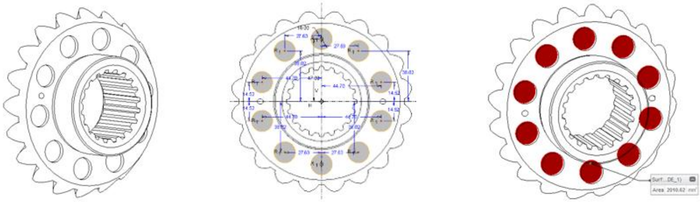

Figure 2.9 Drilling plan with diameter, position and area of the borehole S_k^{bt} on sun gear and differential housing

Friction torque sun gear and differential housing after drilled (2.8).

$$M_{bt/v}^{ms} = \frac{2}{3}\mu_{bt/v}X_{bt}\frac{(r_{tx2}^3 - r_{tx1}^3)}{(r_{tx2}^2 - r_{tx1}^2)} - \frac{\mu_{bt/v}X_{bt}S_k^{bt}r_{tx}}{\pi(r_{tx2}^2 - r_{tx1}^2)} \quad (2.8)$$

From (2.5), (2.8), a graph of the relationship torques on the drive axis M_1=[0÷2000] N.m and friction torque $M_{bt/v}^{ms}$ (Fig 2.24) in case when not drilled and drilled (Fig 2.10).

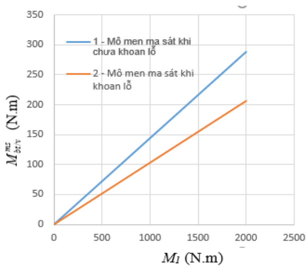

Fig 2.10 Friction torque sun gear and housing when not drilled and drilled

Conclusion Chapter 2

Set up a differential dynamic model and algorithmic scheme takes into account the resistance coefficient of the operating road and the contact friction of the differential components.

Set up a model for calculating friction torque values in differential and solution to change the structure of differential to reduce friction torque.

Chapter 3
SURVEY DYNAMIC DIFFERENTIAL MODEL OF SMALL TRUCKS

3.1. Basic to survey dynamic differential depend on power loss

Along with the gearbox, the rear axle and the differential are studied in the following mainstream tendencies: High torque transmission with highest efficiency and optimal transmission ratio, therefore differential efficiency is an important criterion to evaluate the quality of differential.

We set up a formula to calculate the efficiency of differential (3.1):

$$\eta_{vs} = 1 - \left[l_{ht/tr} + l_{ht/d} + l_{bt/v} \right] \tag{3.1}$$

Inside:

$$l_{ht/tr} = \frac{P_{ht/tr}}{P_2} = \pi . \mu'_{ht/tr} \frac{r_{ct}}{2r_3} \frac{\Delta\omega}{\dot{\varphi}_2} \tag{3.2}$$

$$l_{ht/d} = \frac{P_{ht/d}}{P_2} = \mu_{ht/d} \tan\alpha \sin\delta \left(\frac{\cos(\delta_1 + \delta_0)\sin(\delta_1 - \delta_0) - (\delta_1 - \delta_0)}{\sin(\delta_0 + \delta_1)\sin(\delta_0 - \delta_1)} \right) \frac{r_{ht}}{r_3} \frac{\Delta\omega}{\dot{\varphi}_2} \tag{3.3}$$

$$l_{bt/v} = \frac{P_{bt/v}}{P_2} = \frac{1}{3} \mu_{bt/v} \tan\alpha \sin\bar{\delta} \frac{(r_{tx2}^3 - r_{tx1}^3)}{(r_{tx2}^2 - r_{tx1}^2).r_{tr}} \frac{\Delta\omega}{\dot{\varphi}_2} \tag{3.4}$$

3.2. Investigation the effect of differential friction on differential efficiency LF3070G1 small truck

Based on the system of differential equations describing the dynamics of friction torque in the differential (2.1), (2.2), we have to take the output parameters to calculate transmission differential efficiency.

3.2.1. Investigation original differential model to calculate differential efficiency

- Investigation with torque on the drive axis $M_1=M_e*i_{ht3}$= 320*2.45 N.m
- Case 1 load P=0% weight; Case 2 load P=50% weight; Case 3 load P=100% weight.
- Assume that the road type is agroforestry road has a rolling resistance on the left f=0.14; rolling resistance on the right f=0.12.
- Friction coefficient for all friction positions $\mu=\left[0.03 \quad 0.07 \quad 0.1\right]$.

+ **Case 1:** The efficiency of the highest value differential is η_{vs}= 0.9895 when μ=0.03, η_{vs}=0.9587 when μ=0.07 and η_{vs}=0.9233 when μ=0.1.
+ **Case 2:** The efficiency of the highest value differential is η_{vs}=0.9852 when μ=0.03, η_{vs}=0.9444 when μ=0.07 and η_{vs}=0.8983 when μ=0.1.
+ **Case 3:** The efficiency of the highest value differential is η_{vs}=0.9780 when μ=0.03, η_{vs}=0.9200 when μ=0.07 and η_{vs}=0.8554 when μ=0.1.

3.2.2. Investigation differential structural change to calculate differential efficiency

Calculates the differential efficiency when changing structure η_{vs}^{k} (3.5)

$$\eta_{vs}^{k}=1-\left[l_{ht/tr}^{k}+l_{ht/d}^{k}+l_{bt/v}^{k}\right] \quad (3.5)$$

$$l_{ht/tr}^{k}=\frac{P_{ht/tr}^{k}}{P_2}=\arcsin\left(\frac{l}{r_{ct}}\right).\mu_{ht/tr}^{'}\frac{r_{ct}}{r_3}\frac{\Delta\omega}{\dot{\varphi}_2} \quad (3.6)$$

$$l_{ht/d}^{k}=\frac{P_{ht/d}^{k}}{P_2}=\mu_{ht/d}\tan\alpha\sin\delta\times \quad (3.7)$$
$$\left(\frac{\cos(\delta_1+\delta_0)\sin(\delta_1-\delta_0)-(\delta_1-\delta_0)}{\sin(\delta_0+\delta_1)\sin(\delta_0-\delta_1)}-\frac{S_k^{ht}}{\pi r_{ht}^2\sin(\delta_0+\delta_1)\sin(\delta_0-\delta_1)}\right)\frac{r_{ht}}{r_3}\frac{\Delta\omega}{\dot{\varphi}_2}$$

$$l_{bt/v}^{k}=\frac{P_{bt/v}^{k}}{P_2}=\mu_{bt/v}\tan\alpha\sin\overline{\delta}\left(\frac{(r_{tx2}^3-r_{tx1}^3)}{3r_{tr}(r_{tx2}^2-r_{tx1}^2)}-\frac{S_k^{bt}r_{tx}}{2\pi r_{tr}(r_{tx2}^2-r_{tx1}^2)}\right)\frac{\Delta\omega}{\dot{\varphi}_2} \quad (3.8)$$

Survey with all conditions similar to the original differential

Case 1: Value of differential efficiency $\eta_{vs}^{k}=0.9720$ when μ=0.1.

Case 2: Value of differential efficiency $\eta_{vs}^{k}=0.9636$ when μ=0.1

Case 3: Value of differential efficiency $\eta_{vs}^{k}=0.9508$ when μ=0.1

In the above three case studies, when using the structural change differential when friction coefficient μ=0.1, the maximum differential efficiency increased by 11%.

3.3. Research to improve the dynamics quality of small truck

3.3.1. Theoretical basis to calculate the vehicle traction efficiency

The general formula determines vehicle traction efficiency when traveling straight on the road when it has a different adhesion coefficient between the two wheels (3.9).

$$\eta_k = \eta_{hs}.\eta_{vs}.\eta_{\delta}.100\% \qquad (3.9)$$

Inside:

η_{hs} - Efficiency of gearboxes in transmission and main transmission;

η_{vs} - Differential power transmission efficiency;

η_{δ} - Efficiency considering slip of the active wheels.

3.3.2. Vehicle traction efficiency with low differential locking coefficient

3.3.2.1. Active traction force

- Traction force is calculated according to the torque of the engine is less than the adhension condition of the wheel with the road, ie:

$$P_k = \frac{M_e.i_t\ .\eta_t}{r_{bx}} \le P_{\varphi} = \varphi.Z \qquad (3.10)$$

Inside:

M_e - Torque of the engine;

i_t - Gear ratio of the gearbox number;

η_t - Power transmission efficiency;

r_{bx} - Active wheel radius;

P_{φ} - The adhension force of the active wheels;

φ and Z - Adhesion coefficent and normal reaction force of active wheels.

- Traction force depend on adhension condition.

$$P_k=2.\ \varphi_{min}.\ Z \qquad (3.11)$$

Inside:

φ_{min} - Adhension coefficent of low adhension coefficent wheels.

Compare the P_k value calculated from (3.10) and (3.11). If P_k under (3.10) is smaller than P_k under (3.11), we choose the traction force of the vehicle according to (3.10), whereas we choose the active force of P_k as the force value (3.11)

3.3.2.2. Determine the working mode of the engine

After selecting P_k, we determine the working point of the engine with the M_e torque determined according to (3.12).

$$M_e = \frac{P_k.r_{bx}}{i_t.\eta_t} \qquad (3.12)$$

Based on the engine characteristic curve, we have the number of turns of the crank shalf n_e corresponding to M_e. The angular velocity of the vehicle ω_2 (angular velocity on the differential housing) is given by Equation (3.13).

$$\omega_2 = \frac{\pi.n_e}{30.i_t} \qquad (3.13)$$

3.3.2.3. Determine the slippage of the active wheels

- When adhension coefficient on both sides of the wheel is the same, we can choose sliding δ according to empirical studies. We choose δ= 0.03.

- When adhesion coefficient between two wheels is not equal.

φ_{tr}, φ_{ph} – Adhension coefficient of the left and right wheel $\varphi_{tr} > \varphi_{ph}$. Equilibrium power equation on the two sides of the wheel.

$$M_4\omega_4 = M_5\omega_5 \qquad (3.14)$$

$$\Rightarrow \frac{\omega_5}{\omega_4} = \frac{M_4}{M_5} = \frac{\varphi_{tr}.Z_1.r_{bx}}{\varphi_{ph}.Z_2.r_{bx}} = \frac{\varphi_{tr}}{\varphi_{ph}} = K > 1 \qquad (Z_1 = Z_2, \varphi_{tr} > \varphi_{ph}) \qquad (3.15)$$

Then (3.15) into the basic differential kinetics equation:

$$\omega_2 = \frac{\omega_4 + \omega_5}{2} \Rightarrow \begin{cases} \omega_4 = \dfrac{2\omega_2}{(1+K)} \\ \omega_5 = \dfrac{2K\omega_2}{(1+K)} \end{cases} \tag{3.16}$$

The sliding of the vehicle in straight motion, we have:

$$\delta = \frac{V_{lt} - V_{tt}}{V_{lt}} = \frac{K-1}{K+1} \tag{3.17}$$

Sliding performance is calculated by the formula

$$\eta_\delta = (1 - \delta) \tag{3.18}$$

3.3.3. The vehicle traction efficiency with hight differential locking coefficient

3.3.3.1. Active traction force

- Traction force depend on adhension condition ($\varphi_{tr} > \varphi_{ph}$)

$$P_k = 2\varphi_{ph} Z + K_\delta(\varphi_{tr} - \varphi_{ph})Z \tag{3.19}$$

Choose the traction force similar to the above case

3.3.3.2. Determine the working mode of the engine

If calculate P_k according to (3.12), the drive torque on the differential housing is $M_2 = P_\varphi . r_{bx}$. Similarly determine ω_2 according to (3.13).

3.3.3.3. Determine the slippage of the active wheels

- When adhension coefficient on both sides of wheels is not equal:

We have equations in the high friction differential

$$M_5 = \varphi_{ph}.Z.r_{bx} \tag{3.20}$$

$$M_4 = \varphi_{ph}.Z.r_{bx} + K_\delta(\varphi_{tr} - \varphi_{ph}).Z.r_{bx} \tag{3.21}$$

$$M_2 = P_\varphi.r_{bx} = [2\varphi_{ph} + K_\delta(\varphi_{tr} - \varphi_{ph})].Z.r_{bx} \tag{3.22}$$

$$M_{ms} = M_4 - M_5 = K_\delta(\varphi_{tr} - \varphi_{ph}).Z.r_{bx} \tag{3.23}$$

Similar to the above case:

$$\begin{cases} \omega_4 = \dfrac{2\varphi_{ph}}{2\varphi_{ph} + K_\delta(\varphi_{tr} - \varphi_{ph})}.\omega_2 \\ \omega_5 = 2.\left(1 - \dfrac{\varphi_{ph}}{2\varphi_{ph} + K_\delta(\varphi_{tr} - \varphi_{ph})}\right).\omega_2 \end{cases} \tag{3.24}$$

The sliding of the vehicle in straight motion, we have:

$$\delta = \frac{V_{lt} - V_{tt}}{V_{lt}} = \frac{K_\delta(\varphi_{tr} - \varphi_{ph})}{2\varphi_{ph} + K_\delta(\varphi_{tr} - \varphi_{ph})} \tag{3.25}$$

3.4. Survey results

The LF3070G1 has a working mode of M_{emax}=320 Nm, gear box in number 3 (i_{ht3}=2.45) and has a transmission ratio of main power i_c=6.57.

3.4.1. Effect of low friction differential in traction ability

- The adhension coefficient of the two wheels is not equal

When K_δ=0 (assume φ_{tr}=0.7, φ_{ph}=0.2), P_k=6000.1 N; M_2=2640 N.m, M_4=M_5=1320 N.m; ω_4=9.54 rad/s, ω_5=33.4 rad/s, ω_2=21.47 rad/s; Slippage sharply increased δ=55.56% and efficiency decreased η_k=40.13%.

3.4.2. Effect of hight friction differential in traction ability

- The adhension coefficient of the two wheels is not equal

When K_δ=0.3; traction force P_k=8250 N; M_2=3630 N.m, M_4=2310 N.m, M_5=1320; ω_4=15.14 rad/s, ω_5=26.49 rad/s, ω_2=20.815 rad/s Slippage decreased δ=27.27% % and traction efficiency increased η_k=60.78%.

3.5. Compare traction efficiency between high and low friction differential

At φ_{tr}=0.7, φ_{ph}= [0.1÷0.7]. We have η_k of the differential with low and high friction corresponding to the locking differential K_δ as shown in Figure 3.1.

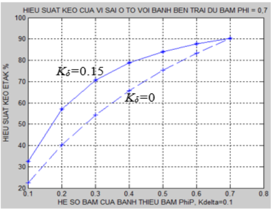

a) Locking differential K_δ=0.15

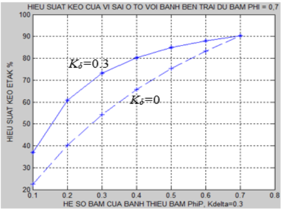

b) Locking differential K_δ=0.3

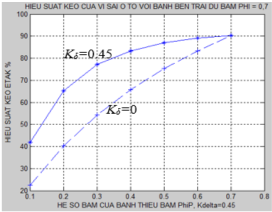

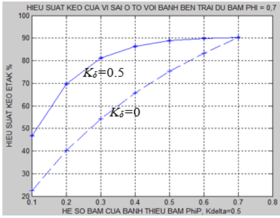

c) Locking differential K_δ=0.45 *d) Locking differential K_δ=0.5*

Hình 3.1 traction efficiency between high and low friction differential

When small trucks work on bad roads, when there is no high friction differential, the angular velocities are much different, while low adhension coefficent wheel will rotate slipping to reduce traction efficiency. Adhension coefficent to the right increases, traction efficiency increases. When the locking differential works, the above defects will be overcome, the slipage of the slip wheel will be reduced, the traction efficiency η_k will increase. In the case of K_δ = 0.3, the torque distributing on the active and the velocity different between two wheels is the most stable, the traction efficiency η_k increased to 14%.

Conclusion Chapter 3

Programming and modeling calculates the differential transmission efficiency through losses due to friction torque of the differential.

Examining the differential efficiency through the friction torque in structural change differential, when using a structural change differential, the differential transmission efficiency increased to the highest of 11 %.

Set up a programming model to investigate the effect of locking differential coefficient K_δ on the differential traction ability.

Chapter 4
EXPERIMENTAL STUDY

4.1. Experimental purpose

The torque musurement at the positions cardan shalf, left and right half-shalfs of three-ton rear axle LF3070G1 truck were assembled in Vietnam when trucks were operating on the agroforestry and on the bench test. In comparison with the results of the distribution of torque on two axles of the vehicle with the torque of distribution on the two axles of the differential dynamics theory taking into account the friction in differential.

4.2. Laboratory equipment and instruments

4.2.1. Rear axle test bench

The experiment using the test bench is the product of the state key research project KC.05.22 / 06-10, fig 4.1.

Hình 4.1 Rear axle test bench

4.2.2. Tenzo

Using FCA-3-11 deformation Tenzo (Fig 4.2) produced by Tokyo Sokki Kenkyjo (Japan) company. Put tenzo on three axes: Cardan axis, two half-shalfs, wiring the sensors into the bridge and wire out.

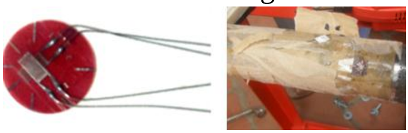

Hình 4.2 Deformation Tenzo use in experiment research

4.2.3. Mercury receiver and wireless transceiver

The experiments used a mercury receiver to obtain the signal from the Cardan shalf and two half-shalfs to measurement device 4.3.

Hình 4.3. Mercury receiver

To obtain the output signal on the rotating axis, a ТРАП-70 mercury receiver was installed on the Cardan shaft and two sets of ТРАП-50 were mounted on the right and left half-shalfs on the test bench. In another embodiment, we use a device with the same functionality as the wireless transmitter of Fig. 4.4.

Hình 4.4 wireless transmitter

4.2.4. Mesuring equipment DMC plus and Spider8

The DMC plus and Spider8 meters are analogous to HBM, Germany, which is used to process low-voltage (<10mV) from tenzo (V_{out}) signals, after amplification. A/D converter is used to make the microcontroller perform the processing, display the measurement process and record the measurement result to a file stored on the computer, Fig 4.5.

Fig 4.5 DMC plus and Spider8 musurement equipment

4.3 Measurement calibration

For the torque musurement work correctly for the structure, size ... the system calibration must be performed. The calibration result is the linear relationship between torque and strain. Perform calibration with mercury receiver and wireless transceiver by generating the torque on the known value, Fig 4.6.

Fig 4.6 Measurement calibration

The sensitivity of the torque sensors is shown in Table 4.1.

Table 4.1: Sensitivity of torque measurements after calibration

Musure equipment	Mercury receiver		wireless transmitter	
	Torque	With	Torque	With
Cardan	750 daNm	2 mV/V	52 kNm	10 V
Left half-shalf	368 daNm	2 mV/V	19 kNm	10 V
Right half-shalf	612 daNm	2 mV/V	26 kNm	10 V

4.4. Proceeding experiments on the test bench

On the cardan shalf put on tenzo at C-1, on two half-shalf put on tenzo at C-2 and C-3. Through the mercury receivers at T-1, T-2 and T-3, the signals from the sensors are sended to the DMC meter, Fig 4.7.

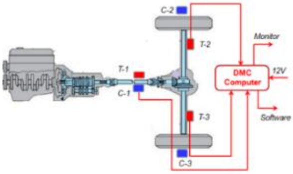

Fig 4.7 Diagram of installation of test equipment on the test bench

4.4.1. Experiment results on the test bench

Figure 4.8 Installing a mercury receiver on the cardan and half-shalf

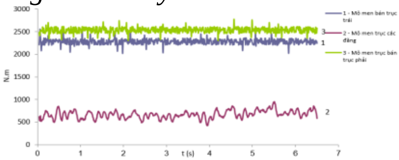

Fig 4.9 Torque on three axes

4.4.2. Compare the results of the experiment on the test bench and calculate from theory

Used the differential dynamic model in Chapter 2 to calculate similar to the experimental conditions on the test bench. Compare the deviation measured results in experiment and calculate by theory Table 4.2.

Table 4.2: Comparison measured torque on the test bench and theoretical calculation

Load	Torque measured (N.m)			Theoretical Torques (N.m)			deviation (%)		
	M_1	M_4	M_5	M_1	M_4	M_5	M_1	M_4	M_5
0%	714.22	2282.73	2632.87	784	2431.03	2683.87	8.9%	6.1%	1.9%
50%	670.82	2062.31	2435.97	726	2258.83	2511.31	7.6%	8.7%	3%
100%	585.96	1794.42	2304.27	637.6	2086.54	2339.37	8.1%	4.7%	1.5%

Rating 1:

The experiment on the test bench is quite close to the assumptions when establishing the differential equation describing the differential dynamics, the measured values compared to the theoretical theory are small. This proves that the set-up model has been approximated to the physical processes that occur in the system.

4.5. Proceeding experiments on smal truck

4.5.1. Experimental truck

The experimental is LF3070G1 truck produced and assembled in Vietnam, the vehicle has an active rear, the self-dumping truck Fig 4.10.

Fig 4.10 Three tons small truck experimental

4.5.2. Diagram of installation of test equipment on the small truck

On the Cardan shalf put on tenzo at T-1 and two half-shalfs put on tenzo at T-2, T-3. Through the wireless transmitter at W-1, W-2 and W-3, the signals from the sensors are sended to the Spider8 meter, Fig 4.11.

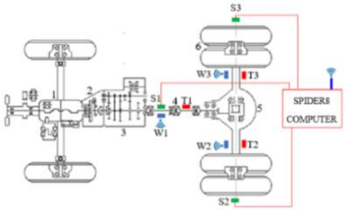

Figure 4.11 Assembly diagram of test equipment on vehicle

4.5.3. Experiment results on light truck LF3070G1 on forest road

Assemble the torque measuring equipment of the cardan and two half-shalf on the vehicle as shown in Fig 4.12.

Fig. 4.12 Assembling of torque measuring equipment

The experimental road is the forest road at Luốt Mountain in Vietnam Forestry University. The results of the torque measurement on the vehicle are shown in Fig 4.12.

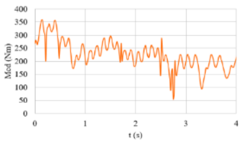

Fig 4.12 Experimental results of cardan torque measurements in vehicle

4.5.4. Compare vehicle measure results and theory simulation calculations

Based on the friction dynamic dynamics model in Chapter 2, the experimental conditions are calculated on the vehicle. Compare the deviation of the measured results in the experiment and calculate the theoretical (Table 4.3).

Table 4.3 Measured results and theoretical calculate

Tải	Torque measured (Nm)			Theorical Torque (Nm)			deviation (%)		
	M_1	M_4	M_5	M_1	M_4	M_5	M_1	M_4	M_5
0%	671.8	2124.73	2329.59	784	2431.03	2683.87	14.3%	12.6%	13.2%
50%	620.73	1962.91	2187.35	726	2258.83	2511.31	14.5%	13.1%	12.9%
100%	543.23	1775.72	2009.51	637.6	2086.54	2339.37	14.8%	14.9%	14.1%

Rating 2:

Due to there are some factors such as vibration vehicles, bumps on the road surface, the longitudinal and horizontal slopes ..., there is a greater deviation than the distribution of torque in theoretical calculation, deviation between the measured value on the vehicle and the calculation from the equation describing the differential dynamics is less than 15%, so the research dynamics model is suitable.

Conclusion Chapter 4

The tenzo sensor is based on the Wheatstone principle of measuring torque of three-axle truck. Design and manufacture fitting tools to mounting measure equipment on three axles when the shafts are rotating at high speed.

Design and manufacture fitting tools to make calibration of torque measuring equipment prior to conducting experiments.

CONCLUSION

1. Building kinetic, dynamical differential model considering friction torque, calculating friction torques. Develop an algorithmic scheme to investigate differential dynamics, determine parameters for differential transmission efficiency.

2. Investigate the case of change in differential structure to change the friction torque M_{ms} in differential, on differential structural change efficiency increased to 11%.

3. The thesis proposes the solution to reduce friction in differential by differential structure change. Thanks to this structural change, the quality of differential differential dynamics increases, small trucks LF3070G1 perform well on agroforestry roads as the vehicle turns.

4. Set up a computational and programmable model to investigate the effect of the K_δ differential lock coefficient on the differential dynamics parameters when the vehicle is working on a bad road. In the case of K_δ=0.3, the traction efficiency η_k increases to 14%, so when the vehicle goes straight on the bad road, the quality of the differential dynamics increases.

5. The experiment uses the tenzo sensor based on the Wheatstone principle, taking the signal simultaneously measuring torque from three rotating axles on rear axle with a mercury contact receiver and a wireless transceiver. The maximum deviation between the measure results on the experimental and the theorical calculation result is 8.9%. The biggest difference between the measured result on the active vehicle and the calculated result is less than 15%. This discrepancy indicates that the differential dynamics model of friction has acceptable reliability.

LIST OF PUBLISHED ARTICLES

1. Nguyen Thanh Quang, **Le Hoang Anh**, Hoang Viet, *Using Inventor Software to Analyze the Kinetics of Active Rear Axle on Light Trucks with locked differential*, ICAT2015, 10/2015, Paper No 10.
2. Nguyen Thanh Quang, Le Hong Ky, **Le Hoang Anh**, *Applying SAE J1266 Standard to Test the Efficiency of Active Rear Axle on Light Trucks*, ICAT2015, 10/2015, Paper No 09.
3. Nguyen Thanh Quang, **Le Hoang Anh**, *Dynamic structure analysis for differential of active rear axle on light truck,* Vietnam Mechanical Engineering Journal 5/2015, ISSN 0866 - 7056, No 5, 5/2016, Page 51 - 57.
4. Nguyen Quang Thai, **Le Hoang Anh**, Đao Duy Trung, Nguyen Thanh Quang, *Dynamic analysis of active rear axle differential on light truck LF3070G1*, National Science and Technology Conference on Automotive Engineering, Hanoi University of Science and Technology, 2016, ISBN 978 - 604 - 95 - 0042 - 08, 10/2016, Page 61- 66.
5. **Le Hoang Anh**, Nguyen Quang Thai, Đao Duy Trung, Nguyen Thanh Quang, *Analysis of torque distribution in differential of light truck active rear axle*, National Science and Technology Conference on Automotive Engineering, 2016, ISBN 978 - 604 - 95 - 0042 - 08, 10/2016, Page 67 - 71.
6. Nguyen Thanh Quang, Hoang Việt, **Le Hoang Anh**, *Thí nghiệm đo mô men xoắn trên cầu sau xe tải nhỏ,* National Science and Technology Conference on Automotive Engineering, National University of Civil Engineering, 2017, ISSN 1859 - 2996, 07/2017, Page 75 - 79.